A connectomics approach to understanding a retinal disease

Charles L. Zucker[a,1], Paul S. Bernstein[b], Richard L. Schalek[c], Jeff W. Lichtman[a], and John E. Dowling[a,1]

[a]Department of Molecular and Cellular Biology, Harvard University, Cambridge, MA 02138; [b]Department of Ophthalmology and Visual Sciences, Moran Eye Center, University of Utah School of Medicine, Salt Lake City, UT 84132; and [c]Center for Brain Science, Harvard University, Cambridge, MA 02138

Contributed by John E. Dowling, June 16, 2020 (sent for review June 5, 2020; reviewed by Alan C. Bird and Dean Bok)

Macular telangiectasia type 2 (MacTel), a late-onset macular degeneration, has been linked to a loss in the retina of Müller glial cells and the amino acid serine, synthesized by the Müller cells. The disease is confined mainly to a central retinal region called the MacTel zone. We have used electron microscopic connectomics techniques, optimized for disease analysis, to study the retina from a 48-y-old woman suffering from MacTel. The major observations made were specific changes in mitochondrial structure within and outside the MacTel zone that were present in all retinal cell types. We also identified an abrupt boundary of the MacTel zone that coincides with the loss of Müller cells and macular pigment. Since Müller cells synthesize retinal serine, we propose that a deficiency of serine, required for mitochondrial maintenance, causes mitochondrial changes that underlie MacTel development.

macular telangiectasia type 2 | serine | Müller cell | macular degeneration | electron microscopy

Little is known about the cellular interactions within the human macula/fovea, the region of the retina mediating high-acuity vision. This is especially true for interactions between retinal glial cells and retinal neurons—interactions likely important for understanding certain retinal degenerative diseases including macular telangiectasia type 2 (MacTel), in which it has been proposed that a defect in the Müller glial cells may be at play (1–3). Müller cells support the functional and structural integrity of the retina by regulating ionic balance and neurotransmission, maintaining metabolic stasis including clearance of waste, and contributing to the blood–retinal barrier, among multiple other essential neuroprotective functions (4, 5).

A recent focus has been on the dependence of retinal neurons on L-serine biosynthesis that occurs in Müller cells and the retinal pigment epithelium (RPE) since retinal neurons (as well as all neurons throughout the brain) lack the rate-limiting L-serine biosynthetic enzyme phosphoglycerate dehydrogenase (PHGDH) (6–8). De novo L-serine synthesis is essential for sphingolipid metabolism and maintenance of mitochondrial structure and function. It also provides the substrate for D-serine and glycine production, among other essential metabolic functions (9–11). Not only have metabolomics studies implicated alterations in the L-serine metabolic pathway in the development of MacTel but genome-wide association studies have linked alterations in the PHGDH gene with early-onset MacTel (12, 13).

MacTel is a relatively uncommon disease affecting a limited region of the central human retina called the MacTel area or zone, which is ∼3 mm (horizontal) by 2.5 mm (vertical), and includes the macula and fovea as well as the nearby parafoveal retina (Fig. 1). Discrete lesions in the MacTel zone cause dramatic losses of visual sensitivity and scotomas in the affected areas. MacTel patients complain of blind spots in their central visual fields as well as metamorphopsia—straight lines appearing wavy or bent. The disease is usually slowly progressive though there are cases where the progression is rapid.

In most cases, outer retinal vascularization is observed, hence the name macular telangiectasia, but it is believed these vascular abnormalities are secondary to loss of retinal neurons and glial cells (14). There is typically in MacTel patients a loss of the yellow macular pigment (Fig. 1) resulting in abnormalities of blue light autofluorescence, as well as the presence of crystals in the inner retina of unknown composition. The retinas also typically show opacities (3, 15).

Several MacTel eyes have previously been studied histopathologically, and a striking finding reported was the loss of Müller glial cells in the MacTel zone (1, 2, 16). These were advanced (and elderly) MacTel patients, so whether this is a general finding is not clear. Despite relatively normal peripheral vision, some abnormalities in the pigment epithelium and subretinal space have also been reported outside the MacTel zone (16, 17).

For the most part, retinal diseases have been characterized by light microscopy. To understand the etiology of a disease, however, we need higher resolution, to look inside cells, examine the cellular organelles, and study the organelles themselves. Many laboratories around the world employing electron microscopy are working to make this possible. One approach to accomplish this is connectomics, the ability to study and reconstruct neural tissue and its component cells. This involves extensive cutting of serial ultrathin (30- to 35-nm) sections, large-scale imaging, and reconstruction of the tissue down to the membrane and organelle level.

We have been applying a high-throughput targeted connectomics methodology for analyzing macular telangiectasia. In brief, being able to cut thousands of sections from large pieces of tissue, several millimeters on a side, allows for the examination of substantial areas of diseased tissue and the identification of regions of interest that then can be reimaged at higher magnification and in depth. By imaging entire sections encompassing the

Significance

Macular degenerations of the retina are a leading cause of legal blindness (visual acuity less than 20/200) globally, and we know little about what causes them. Here we describe electron microscopic observations from the retina of a woman suffering from a rare form of macular degeneration called macular telangiectasia (MacTel). We observed specific changes in mitochondria, the organelle providing energy-rich molecules to cells. The mitochondrial changes likely link to a degeneration of retinal Müller (glial) cells, which we also observed, and serine, an amino acid the Müller cells synthesize which is required for mitochondrial structure and function in all retinal cell types.

Author contributions: C.L.Z. and J.E.D. designed research; C.L.Z., R.L.S., and J.E.D. performed research; P.S.B. and J.W.L. contributed new reagents/analytic tools; and C.L.Z. and J.E.D. wrote the paper.

Reviewers: A.C.B., University College London; and D.B., University of California Los Angeles.

The authors declare no competing interest.

Published under the PNAS license.

[1]To whom correspondence may be addressed. Email: czucker@fas.harvard.edu or dowling@mcb.harvard.edu.

This article contains supporting information online at https://www.pnas.org/lookup/suppl/doi:10.1073/pnas.2011532117/-/DCSupplemental.

First published July 22, 2020.

Downloaded at Palestinian Territory, occupied on November 26, 2021

www.manaraa.com

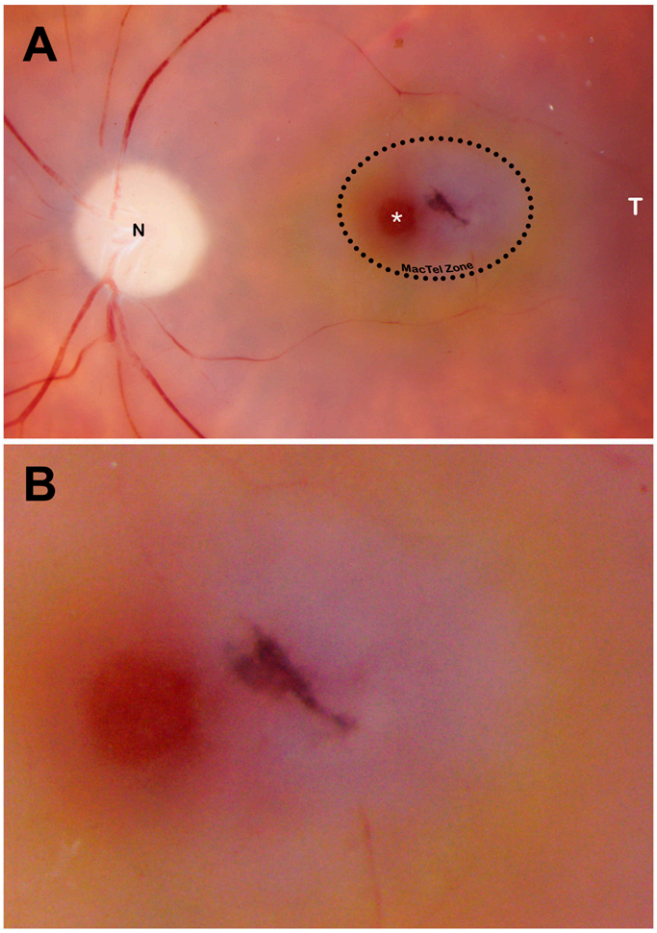

Fig. 1. From ophthalmoscopic postmortem imaging, we are able to visualize the gross features of MacTel in our donor retina. (*A*) The MacTel zone is a region roughly 2.5 mm × 3 mm and encompasses the fovea (∗). Moving temporally (T) from the fovea, a region with a loss of macular pigment includes a pigmented lesion area, a band of prominent macular pigment, and the beginning of a normal-looking area outside the MacTel zone. Note the position of the optic nerve head (N) on the nasal side of the fovea. (*B*) Greater detail of the region from the fovea center to where the macular pigment is retained.

MacTel zone and beyond at intervals of 3 μm, we are able to efficiently generate a three-dimensional representation (*Z* stack) with sufficient resolution to identify and target specific regions and depths for high-resolution analysis. Using these techniques, we have begun to analyze and compare the cellular and organelle integrity and relationships at different retinal depths within, on the border of, and outside the MacTel zone. Although much more needs to be done, we report here some initial observations to emphasize the usefulness of this approach.

Results

From the eye of a woman with MacTel (age 48, who died of cancer), we are examining the macula and perifoveal regions of the retina from one flat-mounted (~3 mm nasal/temporal × 2.5 mm inferior/superior) retinal piece that includes the fovea and extends temporally past the MacTel zone where some pathology occurs. A second piece sectioned radially, several millimeters outside the MacTel zone (perifovea), was also studied. About 10,000 30-nm serial sections of the flat-mounted block were collected on tape for imaging with either a single-beam or high-throughput 61-beam scanning electron microscope (SEM) (18). Overview images of every 100th section were used to determine regions of interest in *X*, *Y*, and *Z* planes to examine at a resolution of 4 nm.

In regions 3 to 5 mm outside of the MacTel zone, the retina appears healthy, both the neurons and their processes as well as the Müller cells (Fig. 2). Although our sections show well-fixed tissue throughout both the outer and inner retina with no sign of anoxia, we do, however, observe abnormalities in a few of the mitochondria in both outer and inner retinal neurons and the Müller cells. These abnormalities consist primarily of striking accumulations of electron-dense material in the mitochondria (Fig. 2 *B* and *C*). On the other hand, we observe many quite normal-appearing mitochondria, so the tissue looks quite capable of supporting normal visual function in line with the experience of MacTel patients (Fig. 2*B*). The prevalence of normal-looking mitochondria only a few millimeters outside the MacTel zone suggests that generalized ischemia prior to fixation, which is known to cause mitochondrial changes (19), was not a significant factor in our tissue, which was fixed ~2.5 h after death. In this paper, we will focus mainly on the outer retina.

In sections closer to the MacTel zone (~1.5 mm away), quite normal-appearing retinal neurons and Müller cells continue to be seen (Fig. 3*A*). The terminals of photoreceptors show invaginations with synaptic ribbons surrounded by synaptic vesicles. Laterally positioned horizontal cell processes and more centrally positioned bipolar cell processes constitute the postsynaptic triad typically observed in central cone terminals (Fig. 3 *A*, *Inset*). However, more prominent mitochondrial pathology is observed in all retinal cells and involves many of the mitochondria. Swelling, reduced numbers of cristae, and internal electron densities are observed consistently within many of the mitochondria (Fig. 3*B*).

In contrast to the perifovea, deep within the MacTel zone, close to the lesion site, the outer retina is profoundly disrupted. Cone terminals appear dense, compressed, and misshapen with the postsynaptic invaginations and triadic complexes disrupted and simplified (Fig. 3*C*). Müller cell processes that typically ensheath the apical surface of the synaptic terminals are missing or greatly swollen and show a denuded cytoplasm devoid of cytoplasmic structure (M in Fig. 3*C*).

Throughout the MacTel zone and in all of the retinal cells, mitochondrial pathology is seen (Fig. 4 and Movie S1). Variations in mitochondrial integrity range from essentially normal to others filled partially or fully with electron-dense material, and yet others swollen with few remaining cristae or internal structure. Some of the mitochondria containing abundant electron-dense material appear to have fused with autophagosomes, forming mitophagosomes and multivesicular bodies which are often found in clusters (Figs. 3*C* and 4*D*).

Pigmented lesions temporal to the fovea and generally in the center of the MacTel zone are often seen as shown in Fig. 1. These lesions may contain intrusive blood vessels, cellular debris, autophagosomes, lysosomes, and unidentified cells (some of which may derive from the RPE) with many defective mitochondria with highly electron-dense internal structures (Fig. 5 *A* and *B*). The electron-dense material in such mitochondria is clearly harder and denser than is the case for normal embedded tissue as shown by the dark horizontal folds caused during sectioning that extend across the structures (Fig. 5*B*). A sharp border between neural elements of the retina and the lesion area is frequently marked by zonula adherens-like structures with associated filamentous material (Fig. 5 *B*, *Inset*) (20).

Henle fibers (the axons that connect the photoreceptor cell bodies with their synaptic terminals) are normally separated from each other by Müller cell processes. Examination of the border of the MacTel zone including a region with macular pigment loss and another with maintained pigment shows there is a sudden and profound change in the normal Müller cell ensheathment of the Henle fibers (Fig. 6). Within the depigmented MacTel zone, Müller cell ensheathment is lost. On the

Downloaded at Palestinian Territory, occupied on November 26, 2021

www.manaraa.com

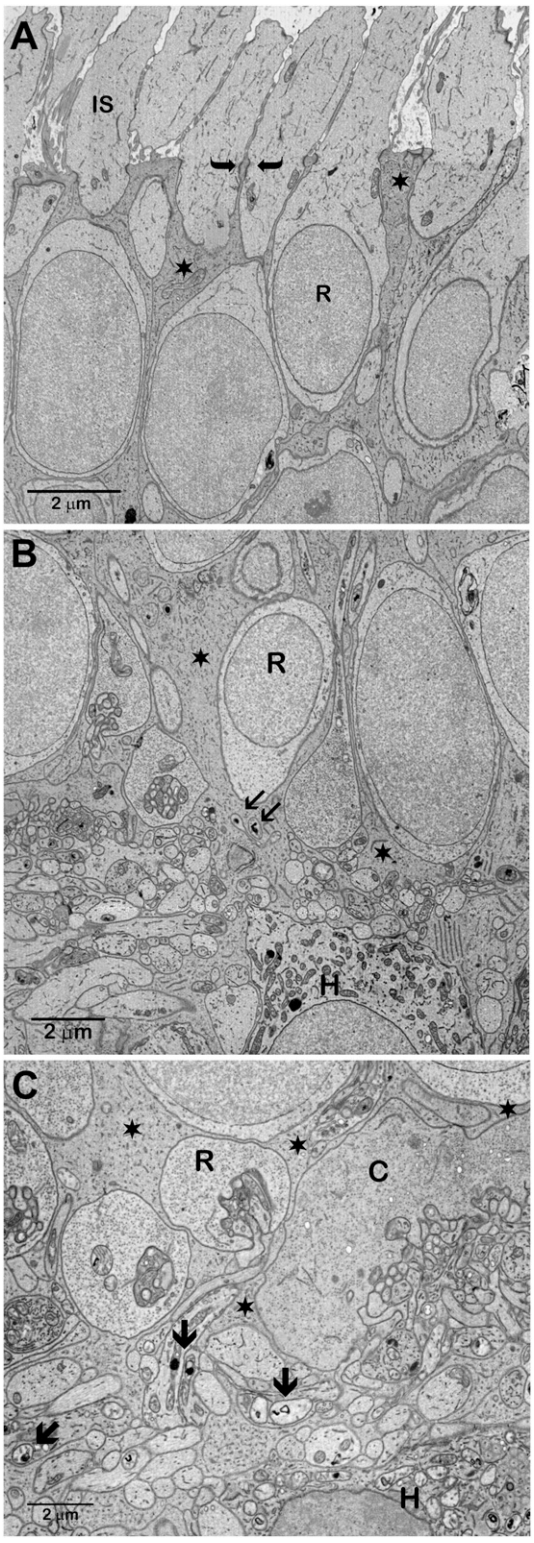

Fig. 2. Well outside of the MacTel zone (3 to 5 mm), cellular and functional relationships appear normal and the tissue preservation is excellent. Rod and cone cell bodies and their terminals (R and C) are surrounded by Müller cell processes (✶) and the Müller cell contribution to the outer limiting membrane (OLM) also appears normal with typical junctions between alternating Müller and photoreceptor cell inner segment (IS) membranes (↪; *A*). However, mitochondria with electron-dense cristae and lightened matrix (arrows) are observed throughout the retina, intermixed with those appearing normal as seen in horizontal cells (H; *B, C*).

other side of the border, where macular pigment is preserved, ensheathment is robust. The border itself is a narrow band of tissue containing cell bodies including those of microglia as well as displaced photoreceptors, cellular debris, and inclusion bodies.

The loss of Müller cell ensheathment in the MacTel zone is also seen clearly proximal to the outer limiting membrane (Fig. 2*A*). Outside the MacTel zone, cone photoreceptor cell bodies are surrounded by three or four Müller cell processes connected by selectively permeable junctions consisting of both tight- and zonula adherens-junctional proteins (21, 22) (Fig. 7*A*), whereas within the MacTel zone only occasional ensheathment is observed of either rod or cone cell bodies (Fig. 7*B*). The locations where these micrographs were taken are indicated in the insets.

In the central region of the MacTel zone, the cone outer segments often show an extraordinary degree of disorder (Fig. 8*A*). The outer-segment discs that normally are neatly stacked and extend out to the plasma membrane are highly vesicularized and disc membranes are often connected in a looping fashion. However, the cone inner segments typically look relatively normal, although many of their mitochondria show densities, swelling, and loss of cristae (Fig. 8*B*).

Discussion

MacTel disease, a rare form of macular degeneration, is of special interest in that there is a well-defined region called the MacTel zone in which lesions appear causing substantial visual disturbances and loss. Whereas some visual changes are known to occur in the perifovea beyond the MacTel zone, good vision is generally retained there, allowing the examination in a single eye of a region with severe visual loss and regions that are relatively normal.

What is known about MacTel is that mutations in genes related to serine synthesis increase the risk of the disease substantially and metabolomics studies indicate decreased levels of serine in patients with MacTel. Further, light microscopic studies indicate degeneration and loss of Müller cells in the MacTel zone and synthesis of retinal serine occurring in the Müller cells.

Our goal here was to determine overall structural changes in a MacTel eye derived from a relatively young patient as well as to examine organelle structure, especially mitochondria, and glial–neuronal relationships involved in MacTel. Most connectomics studies seek to map out comprehensively details of cellular connections within a defined volume. The size of this volume is typically decided upon based on practical or technical limitations—image acquisition time, alignment, segmentation, data storage, and so forth. Such an approach, though capable of providing the extremely rich and saturated data necessary to understand functional neural organization, is impractical to help gain an understanding of neurodegenerative disease processes where sampling over very wide areas and tissue depths is necessary. Further multiple samples (including age- and gender-matched controls) must be analyzed. Our methods for obtaining large numbers of serial sections covering large areas are robust and relatively time-efficient. Imaging of entire sections at relatively low resolution (70-nm *X*, *Y*) at intervals throughout our *Z* depth informs the selection of regions in *X*, *Y*, and *Z* dimensions to image and analyze at 4-nm resolution (or better if deemed necessary). The 70-nm images provide sufficient detail to resolve mitochondria, clearly identify retinal cells and their features (cone pedicles, Henle fibers, etc.), and laminar depth, as well as general properties of retinal integrity and pathology. This effectively gives us a way to explore the MacTel zone and around the foveal region of the retina in all spatial dimensions and at different resolutions.

Perhaps the most informative observations we have made so far are specific mitochondrial changes found in all retinal layers within and outside the MacTel zone. These changes include

Downloaded at Palestinian Territory, occupied on November 26, 2021
www.manaraa.com

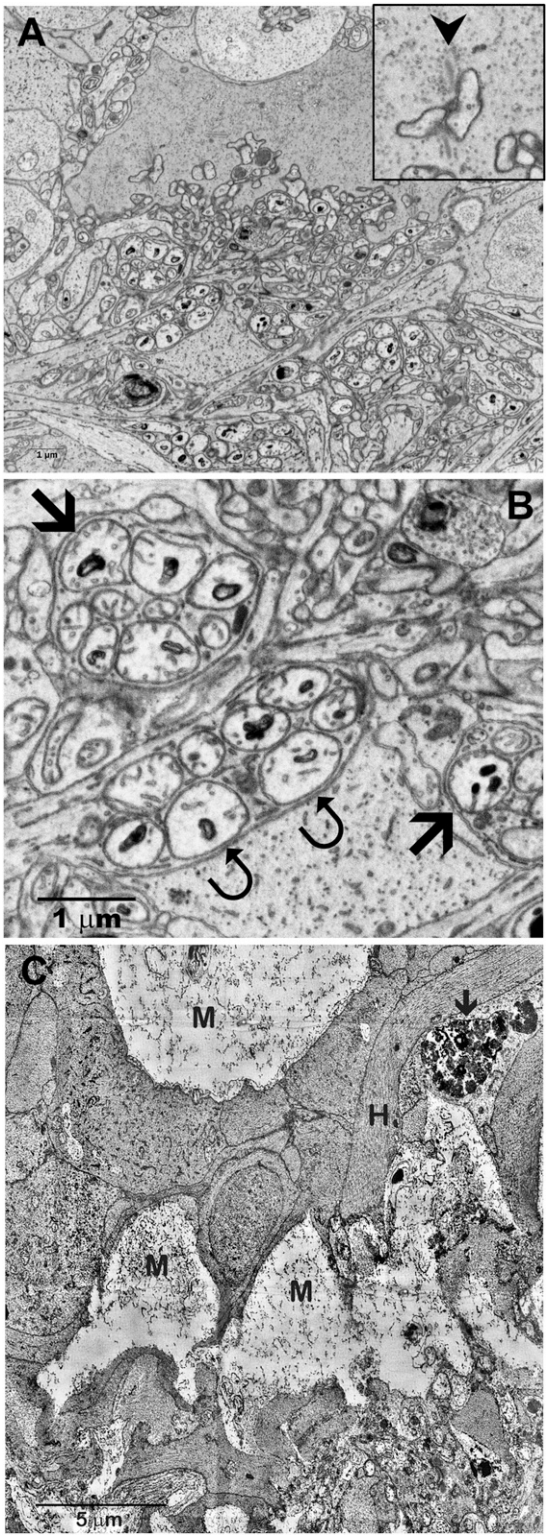

Fig. 3. Defects in mitochondrial structure are seen in the perifovea as well as in the MacTel zone. (*A*) A low-magnification overview image from the perifovea (~1.5 mm from the MacTel zone) shows a cone pedicle with multiple synaptic ribbons surrounded by synaptic vesicles which are adjacent to postsynaptic horizontal and bipolar cell processes (*Inset*, detail from *A*, arrow head). These features demonstrate the fixation quality of our pathological tissue and show the functional circuit motifs that provide the substrate for maintained visual function in these regions, despite the evident mitochondrial defects. (*B*) In perifoveal regions, mitochondria in all cells often show condensed, electron-dense material intermixed with cristae of mitochondria with some condensed electron-dense structures interspersed with normal-looking cristae; mitochondria whose entire contents (matrix and cristae) are filled with electron-dense material, and others that are swollen with extended empty matrix area and few crista fragments; and those in various stages of mitophagy and degradation. Most mitochondria outside of the MacTel zone showing the loss of some cristae appear to retain sufficient structural integrity to suggest maintained function. Interestingly, the outer mitochondrial membranes appear to be more resistant to degeneration than the inner mitochondrial membranes and associated cristae. The outer membranes derive from the endoplasmic reticulum, whereas the inner membranes are where the principal enzymatic reactions occur in the organelle. (*C*) Close to the lesion site, deep within the MacTel zone, the outer retina is profoundly disrupted. Cone terminals appear dense, compressed, and misshapen with the postsynaptic invaginations and triadic complexes disrupted and poorly defined. Müller cell processes that typically ensheath the apical surface of the synaptic terminals and Henle fibers (H) are missing or greatly swollen and show a denuded cytoplasm devoid of cytoplasmic structure (M). Clusters of inclusion bodies containing degrading mitochondria are seen in glial cell processes (arrow).

This is not the first instance that mitochondrial changes have been seen in retinal or neurological diseases (23–25). In instances in which this has been reported, the major findings have been loss of cristae and mitochondrial swelling, and we see similar changes in our material. We are unaware, however, of any instance in which prominent electron-dense cristae have been reported in mitochondria, which we see frequently, especially in regions outside the MacTel area where the rest of the retina appears quite healthy. These electron densities differ in appearance and location from the calcium phosphate inclusions found within the mitochondrial matrix between cristae under conditions of ionic imbalance (26). Within the MacTel zone, where the Müller cells are severely affected, ionic imbalances would also be expected.

Another observation of note is the finding of a discrete border marking the limits of the MacTel zone. Inside the border, intact Müller cell processes are missing for the most part, whereas outside they surround retinal cells and their processes as is seen normally throughout the retina. Inside the border, macular pigment is lacking, whereas it is present outside, providing evidence that the macular pigment resides in Müller cells and their processes, a question long debated (27). Why there is this discrete border is a question that cannot be answered at present. Further analysis of this border through the retinal thickness may provide clues.

Although cones are lost in the center of the MacTel zone, especially near the lesion area, many are preserved, including near the center of the macula. Nonetheless, we often do find significant pathology in the cone outer segments on the lesion (temporal) side of the fovea. Outer segments of healthy cones are filled with well-ordered stacks of visual pigment-containing membranous discs that extend out to the plasma membrane, like a stack of chips in a can. In the MacTel retina, the outer-segment discs rarely extend out to the plasma membrane. Instead, they become extensively vesicularized and fragmented, often showing membranous loops connecting discs distant from each other. As noted earlier, the inner segments of both rods and cones can appear relatively normal when outer segments are showing severe degeneration (Fig. 8), and it is worth noting that inner segments can regenerate outer segments (28). This could explain the reappearance of cones within MacTel lesion areas over time as viewed by adaptive optics (29).

Downloaded at Palestinian Territory, occupied on November 26, 2021

www.manaraa.com

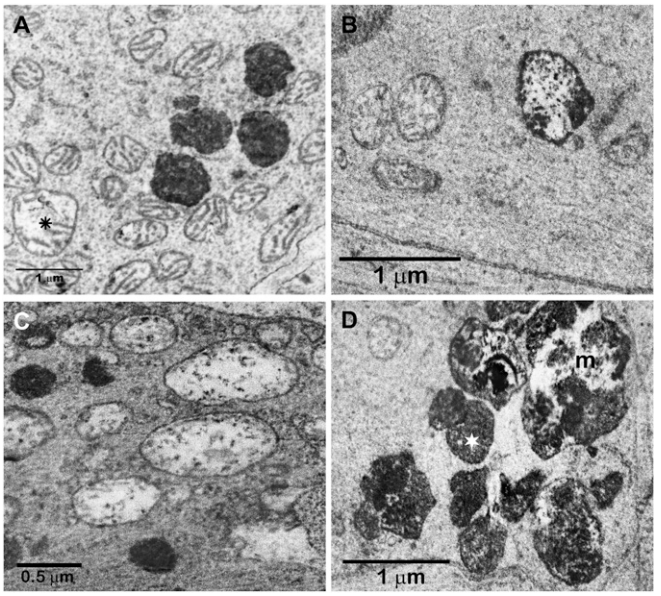

Fig. 4. Variations in mitochondrial pathology in the MacTel zone. (*A*) The ellipsoids of photoreceptors are especially rich in mitochondria. Darkened mitochondria are often seen in the proximal portions of the ellipsoids with the cristae in these mitochondria still discernable within an electron-dense matrix. Swollen mitochondria (∗) are sometimes observed. In this region, structures associated with more advanced stages of organelle degradation, such as phagosomes and lysosomes, are not observed. (*B*) In the proximal portion of Henle fibers, mitochondrial integrity ranges from normal to those containing nearly completely condensed cristae. (*C*) Compared with those outside the MacTel zone, mitochondria within horizontal cell processes in the MacTel zone are swollen with little discernable crista structure. (*D*) Clusters of mitochondria at various stages of degradation are found within some Henle fibers distal to the cone pedicles. This includes electron-dense structures still recognizable as mitochondria (white ∗) as well as mitochondria fusing with phagosomes forming mitophagosomes and multivesicular bodies (m). See also Movie S1 showing a serial stack that includes the areas shown in both *B* and *D*.

Why do the outer segments of the photoreceptors degenerate while the inner segments remain relatively intact? This cannot be answered at the present time, although it might suggest an involvement of the RPE that is so important for the maintenance of the outer segments. Not only does the RPE provide the outer segments with the correct isomer of visual pigment chromophores, it also phagocytoses on a daily basis spent discs of the outer segments. Indeed, outer segments are replaced on a weekly basis to compensate for the phagocytosis of the distal outer-segment discs. Further, it has been proposed that the RPE cells in MacTel are defective in the phagocytic process accounting for the accumulation of outer-segment debris that has been observed between the RPE and outer segments in MacTel retinas (17). In the Royal College of Surgeons rat, such a defect in phagocytosis occurs, and outer-segment material accumulates between the RPE and retina resulting in photoreceptor degeneration (30).

Another possibility explaining outer-segment degeneration is an accumulation of toxic deoxysphingolipids that occurs when serine levels are low. In mice on a diet low in serine, deoxysphingolipids accumulate, resulting in some photoreceptor cell death as well as a reduction in the photopic electroretinogram (12). Since serine is synthesized in both Müller cells and the RPE, the close proximity of the RPE and outer segments might suggest that a loss of locally synthesized serine causes the outer-segment degeneration (13).

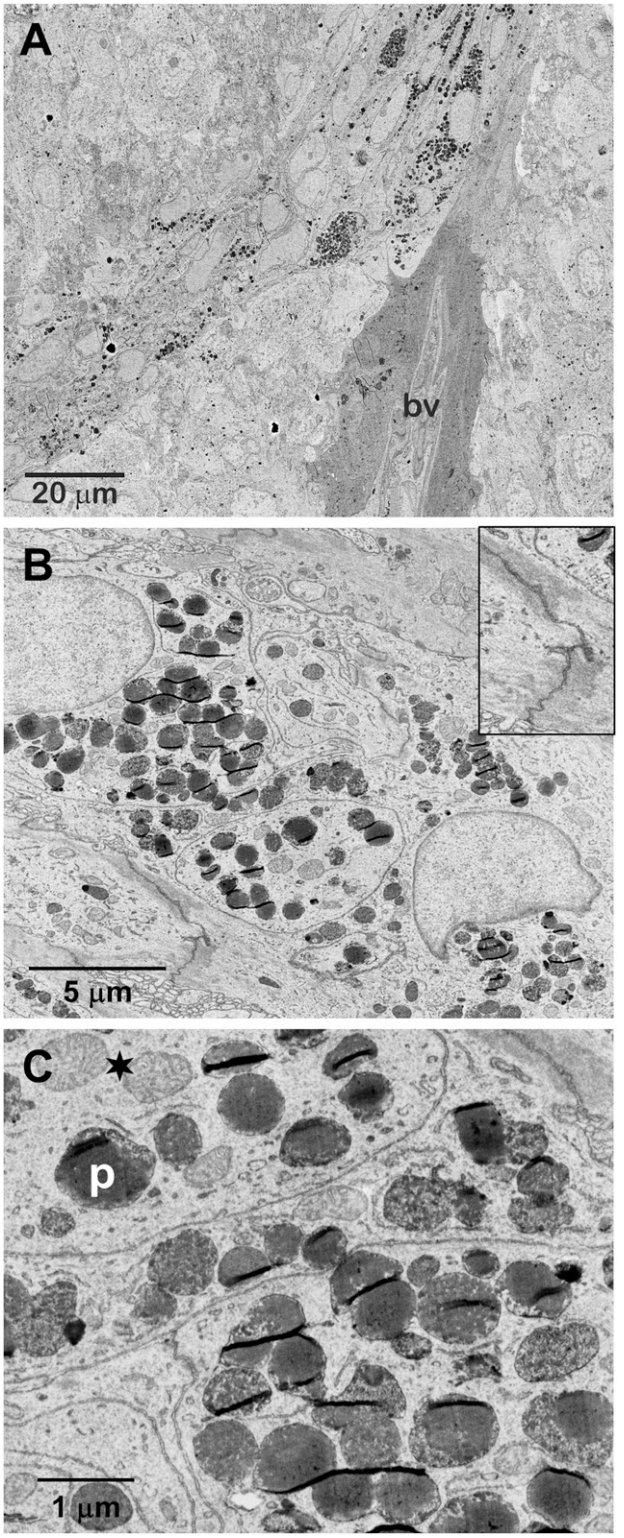

Fig. 5. Mitochondrial structure and degradation are more diverse within the MacTel zone lesion. (*A* and *B*) The lesion area contains a high concentration of electron-dense mitochondria, mitochondria in various stages of degradation via phagocytosis, many pigment granules, and an invading blood vessel (bv). Zonula adherens-like structures with associated filamentous material are often seen at the border between neural elements of the retina and the lesion area (*Inset*). (*C*) At higher magnification, mitochondria of normal appearance (∗) are seen interspersed with those with a dense matrix. Pigment granules (p) are seen as inclusion bodies. The electron-dense material in such mitochondria is clearly harder and denser than is the case for normal embedded tissue as shown by the dark horizontal folds caused during sectioning that extend across the structures.

Downloaded at Palestinian Territory, occupied on November 26, 2021
www.manaraa.com

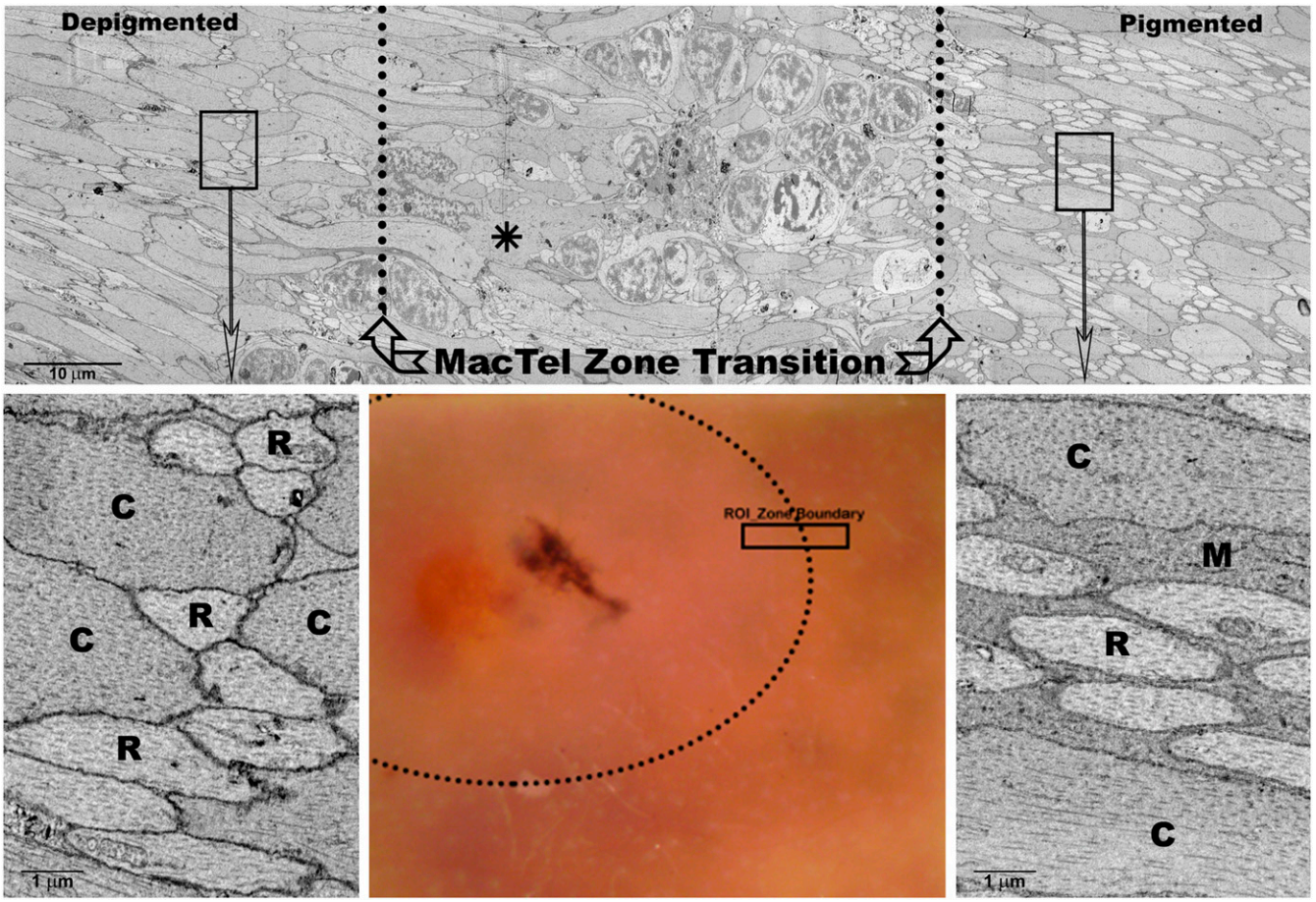

Fig. 6. Region of interest straddling the border of the MacTel zone (color image). (*Top*) Ultrastructurally, a striking demarcation of the MacTel zone is marked by a profound loss of Müller cell ensheathment of the Henle fibers that is maintained on the other side of the border. (*Top Left*) This corresponds to the region observed ophthalmoscopically to be devoid of macular pigment. (*Top Right*) This corresponds to an area still with macular pigment. (*Bottom Left*) The cone (C) and rod (R) Henle fibers are seen directly juxtaposed with each other—without any Müller cell processes surrounding them. (*Bottom Right*) A nearby area just beyond the demarcation zone where the macular pigment has been retained is shown. Here, the cone and rod Henle fibers are fully ensheathed by Müller cell processes (M). A ring of cell clusters is seen separating these two regions along the border of the MacTel zone even though cell bodies are not typically observed in the Henle fiber layer. Ectopic photoreceptor cell bodies (identified by tracing back to connecting Henle fibers) surround a central core of cellular debris. A microglial cell (∗) is also seen extending a process into this core.

A final question is why there is a MacTel area in which the major degeneration occurs (31). Study of foveal structure by connectomics methods (32) revealed that there are two types of Müller cells in the fovea. One is the classic Müller cell that extends from the inner limiting membrane on the inner surface of the retina to the junctions between the inner and outer segments of the photoreceptors (outer limiting membrane). The other cell, called the inner Müller cell, extends only up to the cone pedicles. We do not know as yet the extent of the inner Müller cells across the MacTel zone. Could it be that the inner cells are present throughout the MacTel zone and that they differ in serine synthesis or metabolism, as compared with the classic Müller cell? Such differences could point to why the MacTel zone is a retinal region especially sensitive to a lack of serine.

In summary, we have found that several millimeters outside the MacTel zone, all of the retinal cells look quite normal and healthy, in agreement with the relatively normal vision observed there. However, even here, we see some mitochondria with electron-dense inclusions (Fig. 2). As we move closer to the MacTel zone, the retinal cells still appear reasonably intact and functional, although mitochondrial changes are much more obvious and more numerous (Fig. 3). Within the MacTel zone, we see serious degeneration of the retinal cells, especially the Müller cells, and large accumulations of pathological and degenerating mitochondria that even worsen as we approach the lesion site (Fig. 5). This sequence of alterations indicates that the first observable changes in MacTel are in the mitochondria and suggests that mitochondrial pathology might underlie the MacTel disease because of a deficiency of serine, especially in the central retina, a conclusion consistent with both genetic and metabolomics studies of MacTel retinas.

Materials and Methods

Procurement of a Human Donor Eye. The MacTel eye used in the present study was provided by P.S.B. The donor was a 48-y-old female who died of metastatic uterine leiomyosarcoma ~4 y after being diagnosed with MacTel. We have not been provided with any identifiers associated with the donor other than cause of death and information specific to the retinal disorder. All such information remains with P.S.B. in accordance with all University of Utah privacy of research participants and confidentiality of data protocols.

Tissue Preservation and Initial Processing. The eyes were collected 94 min after death, with the left eye being fully processed and placed into one-half-strength Karnovsky's fixative in cacodylate buffer after a total postmortal time of 2 h, 32 min. The right eye was fixed for light microscopic studies, and sera, plasma, and DNA were also collected. Initial photography and trimming into a Maltese cross occurred prior to our obtaining the tissue. Upon receipt, the tissue, still attached to the sclera, was transferred into fresh half-strength Karnovsky's and stored at 4 °C until further processing.

Downloaded at Palestinian Territory, occupied on November 26, 2021

www.manaraa.com

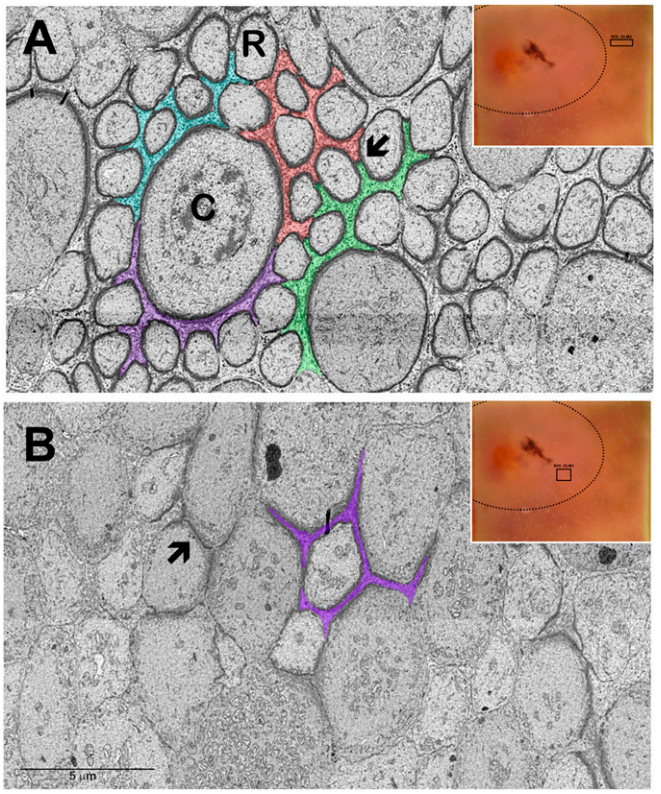

Fig. 7. Müller cell loss in the MacTel zone is seen clearly at the level of the outer limiting membrane. (*A*) Just outside the MacTel zone (see *Inset* for location of image), cone and rod photoreceptor cell bodies (C and R) are surrounded by three or four Müller cell processes (colored) separated by selectively permeable junctions (arrow). (*B*) Inside the MacTel zone, ensheathment is extremely limited, with junctions often directly between photoreceptor inner segments (arrow).

Processing for Serial-Section Electron Microscopy. Following a thorough rinse in ice-cold 0.1 M cacodylate buffer with 0.15 mM $CaCl_2$, the sclera was removed from the retina with still-attached pigment epithelium dissected down to an area of ~3 mm nasal/temporal × 2.5 mm inferior/superior inclusive of the fovea, MacTel zone, and surrounding areas. In order to keep the sample as flat as possible during subsequent processing steps that would normally induce significant curling, we designed a processing chamber in which the retina is held flat while allowing for free exchange of fixatives and other reagents. Within this chamber, the retina is held by sheets of nickel micromesh with a 78% open area (Precision eForming) separated by Teflon spacers equal to the thickness of the retina. The chamber components are also impervious to the reducing agents and other reagents required by the reduced osmium impregnation protocols used to make the tissue electron-dense and conductive. The tissue was stained using a modified ROTO (reduced osmium tetroxide-thiocarbohydrazide-osmium) procedure (33). In brief, the processing chamber with mounted tissue was immersed in reduced osmium tetroxide (1.5% potassium ferrocyanide, 2% OsO_4 in cacodylate buffer) on ice for 1 h. Following washout with distilled water and incubation for 20 min in 1% thiocarbohydrazide at room temperature and a further water rinse, the tissue was incubated for 30 min in 2% aqueous OsO_4. Following washout, the tissue was en bloc stained overnight in 1% aqueous uranyl acetate at 4 °C. Following aqueous washout and a 30-min incubation in Walton's lead nitrate at 60 °C (0.066 g lead nitrate in 10 mL 0.03 M aspartic acid solution, pH 5.5), the tissue was dehydrated up to absolute ethanol prior to removal from the incubation chamber and placed into propylene oxide in preparation for infiltration and flat embedding in Epon between Aclar sheets and then remounted onto a blank Epon block for trimming and sectioning.

Serial Sectioning, Imaging, and Analysis. The tissue was initially trimmed by collecting 1-mm sections that were stained with a methylene blue/toluidine

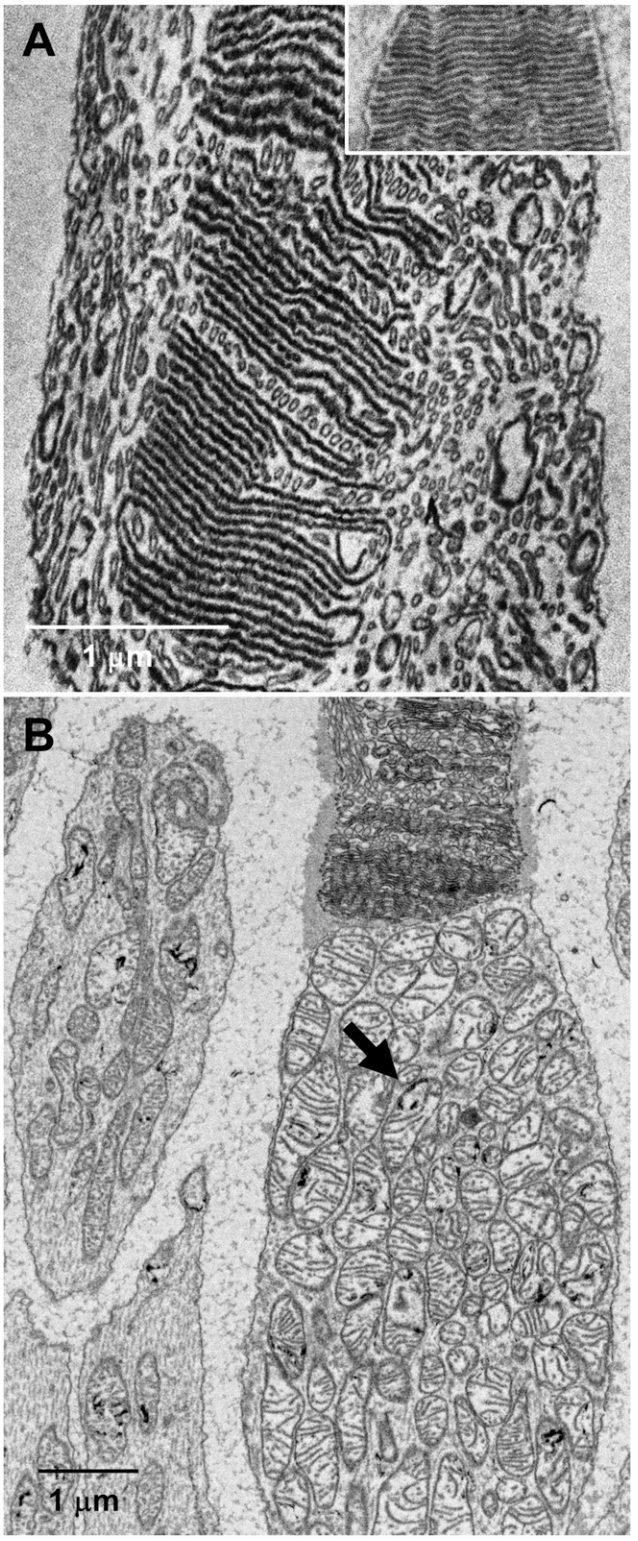

Fig. 8. Cone outer and inner segments in the MacTel zone. Cone outer segment discs are normally highly ordered stacks of membrane that extend out to the plasma membrane of the cell (*Inset*; from outside the MacTel zone). (*A*) Many cones in the MacTel zone, especially those near the center of the macula, show highly disordered disc membranes with extensive vesicularization and fragmentation. Along with discs connected by membranous loops, little association with the outer plasma membrane is seen. (*B*) The apical portion of an ellipsoid of a cone inner segment reveals many mitochondria with isolated electron-dense cristae similar to those seen in the outer plexiform layer outside the MacTel zone (arrow).

Downloaded at Palestinian Territory, occupied on November 26, 2021
www.manaraa.com

blue solution and observed light microscopically to determine the orientation and depth of cutting prior to ultrathin sectioning. Approximately 10,000 serial sections at 30 nm were collected using an automated tape-collecting ultramicrotome (34, 35). Strips of tape containing the serial sections were mounted onto silicon wafers using double-sided carbon tape, and plasma was treated and poststained with uranyl acetate and lead citrate prior to imaging. The first and middle sections from each wafer (each wafer contains close to 200 sections) were imaged in their entirety at an *X*, *Y* resolution of 70 nm by a Zeiss Sigma field-emitting scanning electron microscope to create an overview image stack to facilitate the selection of regions of interest (ROIs). Selected regions in *X*, *Y*, and *Z* positions were then reimaged at 4-nm *X*, *Y* resolution using either a Zeiss Sigma or Zeiss 61-beam MultiSEM depending on the size and *Z* extent of each ROI. Images were stitched and aligned prior to observation and analysis using the volume annotation and segmentation tool [VAST (36)].

Data Availability. Each volume dataset, after image stitching, alignment, and creation of the volume, will be housed on a Harvard server for free access and unfettered use by other investigators after the datasets are completed (available from the corresponding authors). Once a volume is placed on the Harvard site it will be available as an open mineable database. All software and analysis tools developed by the J.W.L. laboratory will be made available to the scientific community upon request.

ACKNOWLEDGMENTS. This work was supported in part by the Lowy Medical Research Institute (J.E.D.), a Macular Foundation grant (to C.L.Z.), NIH Grants U19 NS104653, P50 MH094271, and U24 NS109102-01 (to J.W.L.), and National Eye Institute Grants EY11600 and EY14800 and a Departmental Core Grant from Research to Prevent Blindness, New York (to P.S.B.). We thank Gregory Hageman for the photograph in Fig. 1.

1. M. B. Powner *et al*., Perifoveal Müller cell depletion in a case of macular telangiectasia type 2. *Ophthalmology* **117**, 2407–2416 (2010).
2. M. B. Powner *et al*., Loss of Müller's cells and photoreceptors in macular telangiectasia type 2. *Ophthalmology* **120**, 2344–2352 (2013).
3. M. Okada *et al*., Electrophysiological characterization of macular telangiectasia type 2 and structure-function correlation. *Retina* **38** (suppl. 1), S33–S42 (2018).
4. E. A. Newman, Glial cell regulation of neuronal activity and blood flow in the retina by release of gliotransmitters. *Philos. Trans. R. Soc. Lond. B Biol. Sci.* **370**, 20140195 (2015).
5. E. Vecino, F. D. Rodriguez, N. Ruzafa, X. Pereiro, S. C. Sharma, Glia-neuron interactions in the mammalian retina. *Prog. Retin. Eye Res.* **51**, 1–40 (2016).
6. M. Yamasaki *et al*., 3-Phosphoglycerate dehydrogenase, a key enzyme for L-serine biosynthesis, is preferentially expressed in the radial glia/astrocyte lineage and olfactory ensheathing glia in the mouse brain. *J. Neurosci.* **21**, 7691–7704 (2001).
7. S. Furuya, An essential role for de novo biosynthesis of L-serine in CNS development. *Asia Pac. J. Clin. Nutr.* **17** (suppl. 1), 312–315 (2008).
8. J. T. Ehmsen *et al*., D-serine in glia and neurons derives from 3-phosphoglycerate dehydrogenase. *J. Neurosci.* **33**, 12464–12469 (2013).
9. Y. Hirabayashi, S. Furuya, Roles of L-serine and sphingolipid synthesis in brain development and neuronal survival. *Prog. Lipid Res.* **47**, 188–203 (2008).
10. X. Gao *et al*., Serine availability influences mitochondrial dynamics and function through lipid metabolism. *Cell Rep.* **22**, 3507–3520 (2018).
11. T. Zhang *et al*., Disruption of de novo serine synthesis in Müller cells induced mitochondrial dysfunction and aggravated oxidative damage. *Mol. Neurobiol.* **55**, 7025–7037 (2018).
12. M. L. Gantner *et al*., Serine and lipid metabolism in macular disease and peripheral neuropathy. *N. Engl. J. Med.* **381**, 1422–1433 (2019).
13. T. Sinha, L. Tlkelle, M. Nash, M. R. Al-Ubaidi, The intersection of serine metabolism and cellular dysfunction in retinal degeneration. *Cells* **9**, 674 (2020).
14. I. Leung *et al*.; MacTel Study Group, Characteristics of pigmented lesions in type 2 idiopathic macular telangiectasia. *Retina* **38** (suppl. 1), S43–S50 (2018).
15. F. B. Sallo *et al*.; MacTel Study Group, Abnormal retinal reflectivity to short-wavelength light in type 2 idiopathic macular telangiectasia. *Retina* **38** (suppl. 1), S79–S88 (2018).
16. S. Cherepanoff *et al*., Ultrastructural and clinical evidence of subretinal debris accumulation in type 2 macular telangiectasia. *Br. J. Ophthalmol.* **96**, 1404–1409 (2012).
17. M. B. Powner *et al*., Fundus-wide subretinal and pigment epithelial abnormalities in macular telangiectasia type 2. *Retina* **38** (suppl. 1), S105–S113 (2018).
18. A. L. Eberle *et al*., High-resolution, high-throughput imaging with a multibeam scanning electron microscope. *J. Microsc.* **259**, 114–120 (2015).
19. N. J. Solenski, C. G. diPierro, P. A. Trimmer, A. L. Kwan, G. A. Helm, Ultrastructural changes of neuronal mitochondria after transient and permanent cerebral ischemia. *Stroke* **33**, 816–824 (2002). Correction in: *Stroke* **33**, 1171 (2002).
20. A. Peters, S. L. Palay, H. deF. Webster, *Fine Structure of the Nervous System: Neurons and Their Supporting Cells*, (Oxford University Press, ed. 3, 1991).
21. A. H. Bunt-Milam, J. C. Saari, I. B. Klock, G. G. Garwin, Zonulae adherentes pore size in the external limiting membrane of the rabbit retina. *Invest. Ophthalmol. Vis. Sci.* **26**, 1377–1380 (1985).
22. S. Omri *et al*., The outer limiting membrane (OLM) revisited: Clinical implications. *Clin. Ophthalmol.* **4**, 183–195 (2010).
23. S. J. Baloyannis, V. Costa, D. Michmizos, Mitochondrial alterations in Alzheimer's disease. *Am. J. Alzheimers Dis. Other Demen.* **19**, 89–93 (2004).
24. J. Feher *et al*., Mitochondrial alterations of retinal pigment epithelium in age-related macular degeneration. *Neurobiol. Aging* **27**, 983–993 (2006).
25. C. H. Davis *et al*., Transcellular degradation of axonal mitochondria. *Proc. Natl. Acad. Sci. U.S.A.* **111**, 9633–9638 (2014).
26. J. W. Greenawalt, C. S. Rossi, A. L. Lehninger, Effect of active accumulation of calcium and phosphate ions on the structure of rat liver mitochondria. *J. Cell Biol.* **23**, 21–38 (1964).
27. B. Li *et al*., Imaging lutein and zeaxanthin in the human retina with confocal resonance Raman microscopy. *Proc. Natl. Acad. Sci. U.S.A.* **117**, 12352–12358 (2020).
28. J. E. Dowling, G. Wald, The biological function of vitamin A acid. *Proc. Natl. Acad. Sci. U.S.A.* **46**, 587–608 (1960).
29. Q. Wang *et al*., Adaptive optics microperimetry and OCT images show preserved function and recovery of cone visibility in macular telangiectasia type 2 retinal lesions. *Invest. Ophthalmol. Vis. Sci.* **56**, 778–786 (2015).
30. J. E. Dowling, R. L. Sidman, Inherited retinal dystrophy in the rat. *J. Cell Biol.* **14**, 73–109 (1962).
31. A. C. Bird, D. Bok, Why the macula? *Eye (Lond.)* **32**, 858–862 (2018).
32. D. M. Dacey *et al*., Connectomic reconstruction links human foveal cones to distinct circuitry in the center of the foveal pit. *Invest. Ophthalmol. Vis. Sci.* **58**, 1036 (2017).
33. J. C. Tapia *et al*., High-contrast en bloc staining of neuronal tissue for field emission scanning electron microscopy. *Nat. Protoc.* **7**, 193–206 (2012).
34. K. J. Hayworth *et al*., Imaging ATUM ultrathin section libraries with WaferMapper: A multi-scale approach to EM reconstruction of neural circuits. *Front. Neural Circuits* **8**, 68 (2014).
35. N. Kasthuri *et al*., Saturated reconstruction of a volume of neocortex. *Cell* **162**, 648–661 (2015).
36. D. R. Berger, H. S. Seung, J. W. Lichtman, VAST (volume annotation and segmentation tool): Efficient manual and semi-automatic labeling of large 3D image stacks. *Front. Neural Circuits* **12**, 88 (2018).

Downloaded at Palestinian Territory, occupied on November 26, 2021

www.manaraa.com